

# A new Raman cross section measurement technique monitors the tyrosine environmental dependence of the electromagnetic field strength

Peter J. Larkin, William G. Gustafson, and Sanford A. Asher<sup>a)</sup>

*Department of Chemistry, University of Pittsburgh, Pittsburgh, Pennsylvania 15260*

(Received 11 July 1990; accepted 11 January 1991)

We have developed a new Raman spectroscopic technique which can be used to determine relative Raman intensities as a function of the liquid medium refractive index. We utilize teflon as an external standard. The refractive index dependence of the solid angle of light collection disappears in our sampling geometry and the self-absorption bias is minimized. We observe a refractive index dependence for the Raman intensity for *N*-acetyl-*L*-tyrosinamide (NATYR) close to that calculated using previously derived relations which determine the effect of the refractive index on the electromagnetic field strength and upon the Raman scattered intensities. This dependence gives a ca. 25% increased resonance Raman intensity of NATYR in ethylene glycol compared to water for ca. 243 nm excitation. The strong dependence of the Raman intensity upon the environment suggests that UV resonance Raman intensity measurements can be used to monitor the average environmental refractive index of aromatic amino acids in proteins.

## INTRODUCTION

The investigation of the relationship of Raman intensities to molecular structure and environment has been extensively motivated by the utility of Raman spectroscopy for studying complex systems, especially biological systems such as proteins.<sup>1-15</sup> This is a major factor for the recent development of UV Raman spectroscopy as a probe of aromatic amino acids environments in proteins. For these studies excitation occurs within the aromatic amino acid absorption bands and the resulting Raman frequencies and intensities probe the local environment. Numerous auxiliary studies are required to model the vibrational spectra of the aromatic amino acids in order to characterize the frequency dependence of specific intermolecular or inter-residue interactions such as hydrogen bonding.<sup>15-19</sup> Raman excitation profiles can be used to select excitation wavelengths to resonantly enhance particular aromatic amino acids.<sup>4,10,12,13</sup> These measurements can be used to determine the aromatic amino acid absorption band positions which in turn can be used to obtain information on the local aromatic amino acid environment.

Little use has been made of the measured Raman intensities since absolute intensities are difficult to measure and relative measurements require the use of internal standards.<sup>13,20-25</sup> Changes in the intensity of an analyte Raman band relative to that of an internal standard can indicate a change in the analyte Raman scattering power if the internal standard remains in a well defined environment. However, if the local environments of both the analyte and the internal standard change together, their Raman intensities will change but the observed relative intensities may remain constant. This can occur because the Raman intensities also depend upon the electromagnetic field strength at the scattering molecular site which depends upon the local optical

dielectric constant and resulting refractive index.

The dependence of the Raman intensity upon the local refractive index has been examined theoretically in detail and expressions exist to calculate this dependence.<sup>26-28</sup> A number of visible wavelength Raman measurements have been reported comparing gas phase to solution phase intensities. For some, but not all cases, the agreement between theory and experiment is adequate.<sup>26,28</sup> However, some cases are problematic.<sup>27,28</sup> Furthermore, we recently compared the Raman cross section dispersions of cyclohexane, benzene, and acetonitrile in the gas phase and the liquid phase and found significant conflict between our experimental results and those expected from theory.<sup>29</sup>

In this work we have examined the dependence of the UV resonance Raman intensity of *N*-acetyl-*L*-tyrosinamide (NATYR) upon the environmental refractive index. We have developed a new technique for this study which permits us to easily determine relative Raman intensities by utilizing an external standard, in this case, teflon. We demonstrate that as the environmental refractive index increases, the Raman intensities increase in a manner similar to that theoretically predicted. The Raman intensities of NATYR increase by ca. 25% between pure water and a 90% ethylene glycol: 10% water solution. We discuss the dependence of the Raman intensities on refractive index and the implications of this dependence to aromatic amino acid protein structural studies.

## EXPERIMENT

*N*-Acetyl-*L*-tyrosinamide, NATYR (Sigma Chemical Co.) and spectrophotometric grade ethylene glycol (Aldrich Chemical Co.) were used without further purification. The NATYR solutions were maintained at a high pH (0.07 M KOH) to ensure deprotonation. Approximately 50 ml of sample solution was recirculated through a rectangular stainless steel cell by a magnetic gear pump. A schematic of

<sup>a)</sup> Author to whom correspondence should be addressed.

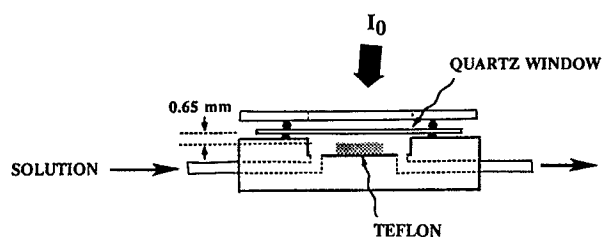


FIG. 1. The cell used for UV Raman measurements. The shaded form is the external standard teflon block (15×5×2 mm). The front window is a Suprasil quartz coverslip sealed with an O ring. The solution sample path length is 0.65 mm.

the cell is shown in Fig. 1. The solution flowed through a 0.65 mm thick rectangular cavity enclosed by a Suprasil quartz window on one side and by a teflon block on the other. The teflon block was used as the external Raman intensity standard for the Raman cross section measurements.

The laser excitation source is a Nd:YAG laser (Quanta Ray DCR-2A) which generates 4–6 ns pulses at a 20 Hz repetition rate. The doubled YAG laser pumps a dye laser (Quanta Ray, PDL) whose output was frequency doubled and mixed with the YAG fundamental to generate 241.6 and 244.5 nm radiation. The laser beam was defocused to a beam diameter of ca. 2 mm at the sample. The pulse energy was measured before and after each Raman measurement using a Scientech Model 361 power meter. In addition, a calibrated photodiode (Hamamatsu S1226-18BQ) was used to continuously monitor the pulse energy flux density. The laser pulse energies were attenuated by placing Suprasil neutral density filters (Melles Griot) in the beam path.

The UV Raman measurements used a 170° backscattering geometry. The Raman scattered light was collected using two quartz spherical lenses at an  $F/\#$  greater than 5.0. However, as discussed below we also made measurements at much larger  $F/\#$ 's by attaching masks to the first lens. The Raman scattered light was focused onto the entrance slit of a Spex Triplemate monochromator. A crystalline quartz wedge placed prior to the spectrometer randomized the polarization of light. The depolarization ratios were measured by placing a Polacoat analyzer prior to the polarization scrambler. A Princeton Applied Research Model 1215 data acquisition console interfaced to a blue-intensified Reticon detector (EG&G PAR Model 1420) was used to detect the dispersed light. The throughput efficiencies of the spectrometer and detector in the UV region were previously determined using a standard intensity deuterium lamp scattered from a Lambert surface prepared from white reflectance standard (Kodak). The instrumentation has been described in greater detail elsewhere.<sup>30</sup>

Ethylene glycol Raman spectra were measured by recirculating ethylene glycol through a 1.0 mm i.d. Suprasil quartz capillary. For these measurements the Raman scattered light was collected in a 135° backscattering geometry using an ellipsoidal mirror.

The NATYR concentrations were adjusted such that the maximum absorbances of the NATYR solution in water

at 241.6 nm and in 90% ethylene glycol: 10% water at 244.5 nm were 0.5 for the 0.65 mm sample path length. The NATYR concentration was 6.76 mM in water and 6.04 mM in 90% ethylene glycol: 10% water. UV Raman excitation of NATYR in water and in 90% ethylene glycol occurred at 241.6 and 244.5 nm, respectively. These conditions ensured that the Teflon external standard was illuminated identically as the incident beam transmitted through the solution volume. We utilized low pulse energy density fluxes for the excitation beam ( $< 1 \text{ mJ/cm}^2$  pulse) to avoid Raman saturation.<sup>14</sup> We extensively characterized the angular dependence of the Raman scattering from the teflon and the NATYR samples. We used a series of masks for the collection lens that transmitted a well defined solid angle about the optic axis, and a series of masks that transmitted a constant solid area but in ringed segments situated at various polar angles relative to the optic axis.

## RESULTS

The observed Raman scattered intensities  $I_a$  for the Raman bands of the dissolved analyte NATYR depend upon a number of factors:

$$I_a = N_a \sigma_a I_0 f_a(\Omega(n)) g_a(A) L_a(n). \quad (1)$$

$N_a$  is the number of molecules of the Raman scattering analyte in the sample solution within the illuminated sample volume collected by the spectrometer collection optics.  $\sigma_a$  is the Raman scattering cross section of the analyte.  $I_0$  is the incident laser intensity into the sample volume.  $f_a(\Omega(n))$  is a factor which specifies the fraction of Raman scattered light collected; it depends on the solid angle of light collection,  $\Omega$ , of the lens which can depend upon the sample refractive index,  $n$ .  $g_a(A)$  is a scaling factor which accounts for the attenuation of the observed Raman scattered light due to self-absorption of the incident and the Raman scattered light by the absorbing medium.  $L_a(n)$  is a correction factor associated with the increase in the Raman intensity for the analyte in the solution compared to that present in the rarefied gas phase. This factor depends upon both the refractive index of the analyte and of the sample solution and derives from the increase in the electromagnetic field strength in a dielectric environment compared to that present in vacuum. This expression is also valid for the Raman scatterers water and ethylene glycol solvent medium.

A similar expression can be written for the observed Raman scattering intensity of the teflon Raman bands:

$$I_T = N_T \sigma_T I_0 f_T(\Omega(n)) g_T(A) L_T. \quad (2)$$

The subscript  $T$  is used to clearly differentiate the teflon factors from those of the analyte contained in solution. One reason for this distinction is that the local field correction for the teflon is constant and independent of the solution refractive index. Furthermore, the self-absorption factor for teflon differs from that of the analyte since all of the teflon Raman scattered light must traverse the entire sample solution while the analyte scattering occurs from molecules situated throughout the illuminated sample volume.

The teflon Raman scattered light derives from Raman scattering from the bulk teflon. However, all of the Raman

scattered light can be thought of as radiating directly from the surface of the teflon due to the complete multiple scattering which occurs over micron thin thicknesses. We have examined the scattering of teflon in the UV and find that negligible absorption is present for ca. 243 nm light, but that the light is completely multiply scattered by extremely thin thicknesses of less than 0.025 mm. In fact, this multiple scattering results in observed depolarization ratios of 1.00 for the teflon Raman bands. Because this intense diffuse scattering phenomena can show anomalous angular dependencies we expected that  $f_T(\Omega(n))$  would differ significantly from  $f_a(\Omega(n))$ .<sup>31</sup>

Given the same analyte molecule present in two different solvents with two different refractive indices,  $n_1$  and  $n_2$ , the ratio of the local electromagnetic field correction factors is given by Eq. (3) where we can experimentally determine each of the factors.

$$\frac{L_a(n_2)}{L_a(n_1)} = \frac{(I_A/I_T)_2}{(I_A/I_T)_1} \left( \frac{f_a(\Omega(n_1))}{f_T(\Omega(n_1))} \right) \left( \frac{f_T(\Omega(n_2))}{f_a(\Omega(n_2))} \right) \times \left( \frac{g_a(A_1)}{g_T(A_1)} \right) \left( \frac{g_T(A_2)}{g_a(A_2)} \right) \frac{N_{a1}}{N_{a2}} \quad (3)$$

the ratio of the intensity of the analyte, NATYR, to the external standard, teflon, in the two solvents of differing refractive indices can be directly measured. The ratio of the two analyte concentrations gives us the ratio  $N_{a1}/N_{a2}$ .

The ratio of the angular dependencies of the ratio of the Raman intensities of the analyte to the external standard

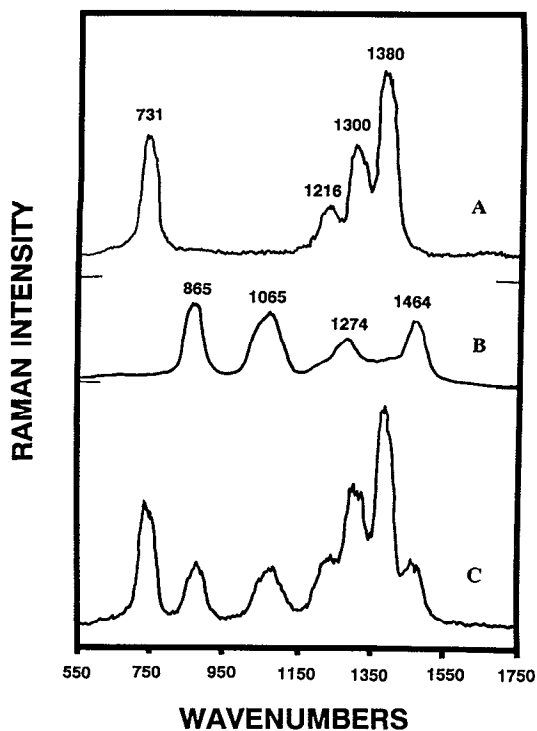


FIG. 2. UV Raman spectra at 241.6 nm of (A) teflon in cell with water in cavity; (B) pure ethylene glycol in a Suprasil quartz capillary; (C) teflon in cell with ethylene glycol in cavity.

must be determined experimentally. Figure 2(A) shows the Raman spectrum of teflon using 241.6 nm excitation obtained with water in the cell. Four distinct teflon bands are observed at 731, 1216, 1300, and 1380  $\text{cm}^{-1}$ . Figure 2(B) shows the Raman spectrum of ethylene glycol in a capillary using 241.6 nm excitation. Bands are observed at 863, 1065, 1274, and 1464  $\text{cm}^{-1}$ . Figure 2(C) shows the UV Raman spectrum of ethylene glycol and teflon in the cell shown in Fig. 1 using 241.6 nm excitation.

Figure 3(A) shows the dependence of the 731  $\text{cm}^{-1}$  teflon band intensity as a function of the collected solid angle for the situation where either water or a 90% ethylene glycol–10% water solution fills the space between the teflon and the quartz window. We also measured the angular dependence of the intensity with air in the cell. For all cases the intensity decreases as the average polar collection angle increases. The observed decrease in intensity derives from the convolution of the angular decrease in the Raman scattered intensity and the angular decrease in the transfer function of the collection optics-spectrometer system.

Figure 3(B) shows the angular dependence of the ratio of the 731  $\text{cm}^{-1}$  band intensity with water in the cell versus ethylene glycol solution in the cell. Similarly, Fig. 3(C) shows the angular dependence of the teflon 731 and 1380

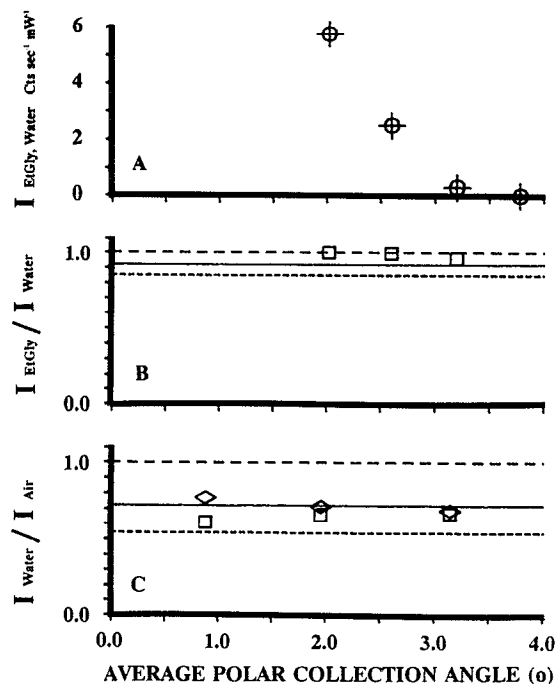


FIG. 3. Angular dependence of the Raman intensities of teflon with 241.6 nm excitation. (A) Intensity of teflon 731  $\text{cm}^{-1}$  band with water (cross) and with 90% ethylene glycol: 10% water (circle) in the cavity. (B) The teflon 731  $\text{cm}^{-1}$  band intensity ratio with water vs 90% ethylene glycol solution in the cavity. The data in (A) and (B) were obtained with constant area ( $7.38 \times 10^{-3}$  sr) annular ring masks at various polar angles about the optic axis. (C) The intensity ratios of the teflon 731  $\text{cm}^{-1}$  band (square) and 1380  $\text{cm}^{-1}$  band (diamond) with water vs air in the cavity. The data in (C) derive from difference spectra obtained using circular apertures of increasing solid angle. The horizontal lines in parts (B) and (C) show the intensity ratio expected for refractive index dependences of  $1/n^2$  (short dash) and  $1/n$  (solid).

$\text{cm}^{-1}$  band intensity ratios for water vs air in the cell. These angular dependences were determined by inserting various circular and annular apertures on the first collection lens situated 23 cm from the sample cell. The data of Fig. 3(B) were obtained from spectra measured using annular apertures with a constant solid angle of  $7.38 \times 10^{-3}$  sr; these annular segments were situated at average polar angles between  $2^\circ$  and  $4^\circ$ . The Fig. 3(C) data were measured by using circular apertures of increasing solid angle. The data at different average angles were obtained by subtraction of spectra obtained with different circular apertures.

For the typical light collection geometry the solid angle of light collection is expected to vary as  $1/n^2$  due to refraction in the sample medium.<sup>34-37</sup> Given a refractive index of 1.39 for water<sup>32</sup> and 1.00 for air at 241 nm, we calculate that the ratio of the solid angle collected with water in the cell vs air to be equal to 0.52. If the teflon scattering intensity is uniform over the angles collected this should translate to an intensity ratio of 0.52 for water versus air in the cell. Figure 3(C) clearly shows that the intensity ratio is independent of the average polar solid collection angle. Furthermore, the observed ratio, in contrast to our expectation, is close to a  $1/n$  dependence (0.72). Figure 3(B) shows the observed intensity ratio for water in the cell vs ethylene glycol solution. Given a calculated 90% ethylene glycol solution refractive index at 241 nm of 1.51 (the refractive index of pure ethylene glycol is unknown for 241 nm light, but we estimate it to be 1.53 from the data for glycerol<sup>33</sup>), we calculate a ratio of 0.85 for a  $1/n^2$  collection angle dependence. In contrast, we observe a ratio close to 1.00; however, the signal-to-noise of the data do not rule out an experimental ratio of 0.92 (the expected value for a  $1/n$  dependence of the solid angle collected). The independence of the intensity ratio of teflon scattering with collection angle is consistent with the multiple scattering teflon block acting as a diffuse Lambert surface type scattering source.

The observed ca.  $1/n$  dependence of the teflon Raman scattering intensity on the solution refractive index is inconsistent with the often quoted  $1/n^2$  dependence of the observed collected light intensity.<sup>34-37</sup> The  $1/n^2$  factor derives from the expected refraction change in the solid angle of light collected from within the sample, relative to that in air. The original derivation by Hermans and Levinson<sup>34</sup> was calculated for fluorescence from a diffusely and uniformly illuminated sample where the slit image within the sample volume was small compared to the illuminated area, but the illuminated volume was thin. The calculation ignored any aberrations in the collection efficiencies. More recent studies have extended the  $1/n^2$  dependence to geometries with larger slits and larger illuminated volumes of the sample.<sup>36,37</sup> Indeed, Schomacker *et al.*<sup>23</sup> in a recent study clearly observe a  $1/n^2$  dependence for teflon Raman scattering for a teflon rod within a fluorescence cuvette containing air, water or benzene. However, the general validity of this angular dependence has been questioned.<sup>38</sup>

For our sample geometry we uniformly illuminate a broad area of sample. The optical path length is very thin. Because of the large size of the illuminated area object, there may be significant aberrations arising from imaging into the

$400 \mu\text{m}$  entrance slit which may dominate the optical transfer function from the sample object through the entrance slit. For our experimental geometry, it is clear that there is ca.  $1/n$  dependence of the teflon Raman intensities upon the solution refractive index. Similarly, the analyte Raman bands should also show this  $1/n$  dependence upon solution refractive index. Thus, the ratios of both the analyte and teflon external standard angular dependent collection efficiency factors for the two refracting media will be equal

$$\frac{f_a(\Omega(n_1))}{f_a(\Omega(n_2))} = \frac{f_T(\Omega(n_1))}{f_T(\Omega(n_2))}$$

and the product of the analyte and teflon angular dependent collection efficiency ratios in Eq. (3) will be unity.

The sample self-absorption factors in Eq. (3) are experimentally determined by measuring the relative attenuation of the teflon and ethylene glycol bands by the absorbing NATYR solutions. The small sample thickness used minimizes the self-absorption correction. The sample solution concentrations were adjusted to identical absorbance values such that identical relative laser intensities are incident upon the teflon block. Figure 4 shows the absorption spectrum of NATYR under alkaline conditions in both water and 90% ethylene glycol: 10% water. NATYR has an absorption maximum at 241.4 nm in water, and a calculated molar absorptivity of  $11.55 \text{ cm}^{-1} \text{ mM}^{-1}$ . The 241.4 nm peak maximum of NATYR in water is found to redshift to 244.0 nm in the ethylene glycol solution. We observe an increase in the calculated molar absorptivity to  $12.98 \text{ cm}^{-1} \text{ mM}^{-1}$ , as well as a decrease in the absorption bandwidth.

Despite the identical absorbances of the NATM samples at the two excitation wavelengths chosen, the effect of self-absorption on the ethylene glycol and external standard teflon bands must be characterized for both excitation wavelengths. This is required because of the different bandshapes of the absorption band of NATYR solution in water and in the 90% ethylene glycol solution. The UV Raman spectra of NATYR in water with 241.6 nm excitation and NATYR in 90% ethylene glycol with 244.5 nm excitation are shown in Fig. 5. The tyrosinate band at  $1601 \text{ cm}^{-1}$  is clearly observed as are the ethylene glycol and teflon bands. As a result of self-

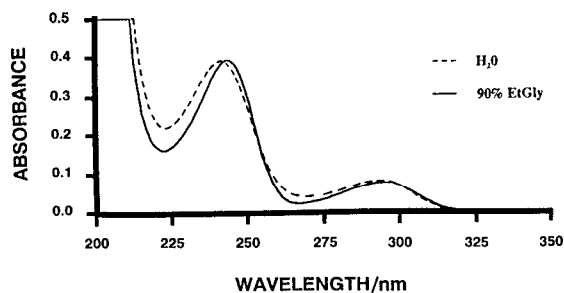


FIG. 4. UV absorption spectra of deprotonated *N*-acetyl-*L*-tyrosinamide (NATYR, 0.07 M KOH) in an aqueous solution (6.76 mM NATYR, dashed line) and in a 90% ethylene glycol: 10% water solution (6.04 mM NATYR, solid line). The sample cell path length is 0.5 mm.

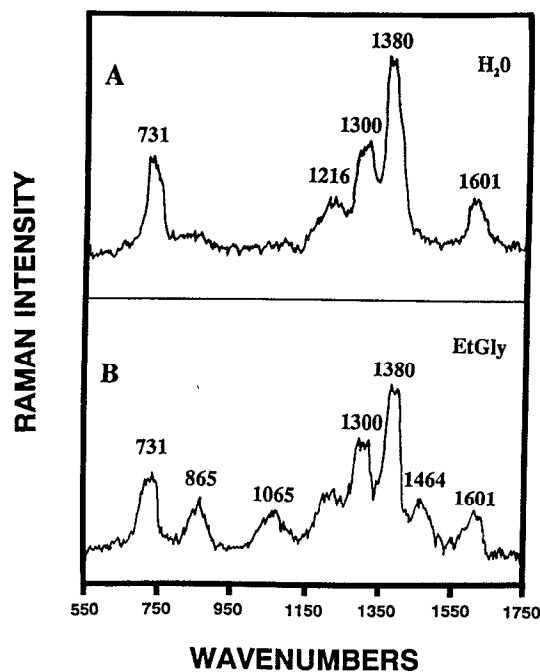


FIG. 5. Resonance Raman spectra of *N*-acetyl-*L*-tyrosinamide (NATYR, 0.07 M KOH): (A) NATYR in aqueous solution in cell excited at 241.6 nm with teflon as external standard; (B) NATYR in 90% ethylene glycol: 10% water solution in cell excited at 244.5 nm with teflon as the external standard. The absorbances of the two NATYR samples were identical at their respective excitation frequencies.

absorption, there is a dramatic decrease in the absolute and relative Raman intensities of the teflon and ethylene glycol bands in the presence of NATYR.

Figure 6 plots the relative self-absorption correction factors for both water and 90% ethylene glycol NATYR samples. These factors can be used to rescale the relative intensities of ethylene glycol and teflon bands in the presence of NATYR to those which would occur in the absence of self-absorption. Clearly the slopes are identical, and thus, the ratio of the absorption correction factors in Eq. (3) becomes unity for our sample geometry.

Given the measured relative Raman intensities for NATYR relative to teflon for the water and 90% ethylene glycol solutions, the relative concentrations and the estimated uncertainties associated with the deviations of the angular and absorption factors in Eq. (3), we calculate  $L_{\text{etgly}}/L_{\text{water}} = 1.28 \pm 0.08$  (relative standard deviation of ca. 6%).

## DISCUSSION

The response of molecules to electromagnetic radiation depends upon the electromagnetic field strength. As indicated in Eq. (3) the Raman intensity scales with the local field correction factor,  $L$ , which depends upon the refractive index. The detailed expression for the local field correction factor is based upon classical electromagnetic theory which relates the electromagnetic field strength through a continuum dielectric model to the medium refractive index and the refractive index of the analyte molecule.<sup>39-41</sup> The dielectric

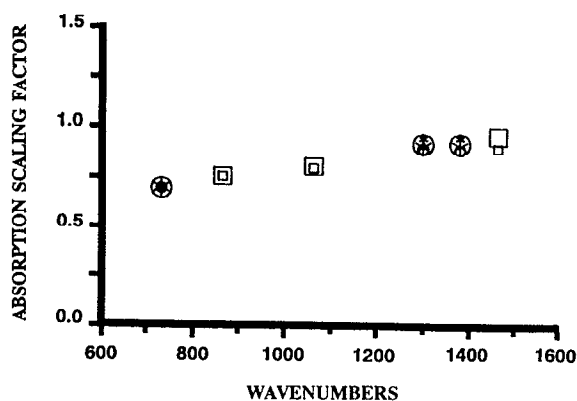


FIG. 6. Comparison of the relative self-absorption correction factors for teflon and ethylene glycol bands resulting from NATYR (0.07 M KOH) absorbances. Circles: teflon bands using 241.6 nm excitation of aqueous NATYR solution. Asterisks: teflon bands using 244.5 nm excitation of 90% ethylene glycol: 10% water NATYR solution. Squares: ethylene glycol bands using 244.5 nm excitation of 90% ethylene glycol: 10% water NATYR solution. Small symbols: from measurements using a solid collection angle of 0.007 44 sr. Larger symbols: from measurements using a solid collection angle of 0.0312 sr. The curves were normalized such that the 731  $\text{cm}^{-1}$  teflon Raman band relative absorption scaling factors were identical.

continuum is polarizable and responsive to changes in the polarization of the analyte molecule induced by the incident electromagnetic radiation. The probability for absorption and Raman scattering is intimately dependent upon the electromagnetic field strength as scaled by the dielectric constant of the surrounding medium.

The appropriate form of the local field expression that should be applied to measured Raman cross sections and absorbances of solutions remains the subject of debate.<sup>22,26-28,42</sup> However, the informative thesis of Nestor<sup>28(b)</sup> compares the different approaches and concludes that the Eckhardt and Wagner<sup>26</sup> approach is the most theoretically sound, as well as in best agreement with the available experimental data. This simple model ascribes the dependence of the absorbance and the Raman cross sections to differences in the refractive indices of the pure analyte and the local environment.<sup>26-28</sup> The expression for the increased electric field strength of a molecule in the neat liquid phase compared to that of the same molecule in the gas phase for absorption is given as

$$\frac{A_l}{A_g} = \frac{1}{n} \left( \frac{n^2 + 2}{3} \right)^2, \quad (4)$$

where  $A_l$  and  $A_g$  are the integrated molar absorption coefficients in the liquid and gas phases, and  $n$  is the refractive index of the neat liquid. The ratio of the maximum molar absorptivities is identical to the ratio of Eq. (4) if identical absorption band shapes exist in the gas and liquid phases.

The analogous expression for Raman scattering for the gas and neat liquid phase is given as

$$\frac{S_l}{S_g} = \frac{n_l'}{n_i} \left( \frac{n_l'^2 + 2}{3} \right)^2 \left( \frac{n_i'^2 + 2}{3} \right)^2 \approx \left( \frac{n^2 + 2}{3} \right)^4, \quad (5)$$

where  $S_l$  and  $S_g$  are the Raman scattered intensities of the

analyte in the liquid and gas phase, and  $n_l$  and  $n'_l$  are the refractive indices at the excitation and Raman scattered frequencies, respectively. If  $n_l = n'_l$  the expression significantly simplifies.

The local field expression which relates the relative absorbances for an analyte molecule in a solvent environment to the same molecule in the gas phase is more complex. The expression for the absorption of the analyte is given by Rea<sup>43</sup> as

$$\frac{A_s}{A_g} = \frac{1}{n_s} \left( \frac{n^2 + 2}{(n/n_s)^2 + 2} \right)^2, \quad (6)$$

where  $n$  and  $n_s$  are the refractive indices of the pure liquid and the solution at the excitation frequency, respectively.

In contrast to Rea's<sup>43</sup> work and that of Mirone<sup>27</sup> the most likely correct ratio of Raman intensities is given by Eckhardt and Wagner:<sup>26</sup>

$$\frac{S_s}{S_g} = \frac{n'_s}{n_s} \left( \frac{n_s^2 + 2}{3} \right)^2 \left( \frac{n'^2_s + 2}{3} \right)^2 \cong \left( \frac{n_s^2 + 2}{3} \right)^4, \quad (7)$$

where  $n'_s$  is the refractive index of the solution at the Raman scattered frequency. Typically, the small refractive index differences between the incident and Raman scattered light are neglected and the right-hand expression is used. However, if the refractive index shows dispersion (such as within an absorption band) the approximate expression could lead to significant errors.

The expressions that give the ratio of absorbances and Raman intensities for an analyte between two solutions of different refractive index are given as

$$\frac{A_1}{A_2} = \left( \frac{n_1}{n_2} \right)^3 \left( \frac{n^2 + 2n_2^2}{n^2 + 2n_1^2} \right)^2 \cong \frac{L_a^4(n_2)}{L_a^4(n_1)}, \quad (8)$$

$$\begin{aligned} \frac{S_1}{S_2} &= \frac{n'_1 n_2}{n_1 n'_2} \left( \frac{n_1^2 + 2}{n_2^2 + 2} \right)^2 \left( \frac{n_2^2 + 2}{n_1^2 + 2} \right)^2 \\ &\cong \left( \frac{n_1^2 + 2}{n_2^2 + 2} \right)^4 \cong \frac{L_a^R(n_2)}{L_a^R(n_1)}, \end{aligned} \quad (9)$$

where the subscripts refer to the two different solution environments, and  $L_a^A(n)$  and  $L_a^R(n)$  are the absorption and Raman local field correction factors. Equations (8) and (9) present the local field ratio for solutions of differing refractive indices. Utilizing expressions (8) and (9) we can calculate the local field contributions and compare the results to our experimental observations.

The measured refractive index of water<sup>32</sup> at 241 nm is ca. 1.39. Although the UV refractive index of ethylene glycol has not been measured, a structurally similar species, glycerol has a refractive index of 1.56 at 241 nm.<sup>33</sup> We estimate the refractive index of the 90% ethylene glycol: 10% water solution at 241 nm to be 1.51. Estimation of the refractive index of NATYR at 241 nm is more difficult. Electron rich conjugated molecules can show refractive indices of 1.8 in the UV spectral region and exhibit strikingly large variations in their refractive indices within an absorption band.<sup>44,45</sup> As a first approximation we estimate the refractive index of NATYR at 241 nm to be 1.8.

Using an estimated refractive index of 1.8 for NATYR,

a refractive index of 1.51 for a solution of NATYR in 90% ethylene glycol: 10% water and a refractive index of 1.39 for a solution of NATYR in water, we obtain a value of 1.06 for the relative ratio of the integrated absorbances of NATYR in ethylene glycol vs water. This ratio compares favorably to the 1.12 value which we observe for the ratio of the maximum molar absorptivity values. The calculated local field ratio will be even closer to the observed absorbance ratio if the integrated molar absorptivities are used since the bandwidth of NATYR in 90% ethylene glycol: 10% water is decreased. An integrated oscillator strength ratio greater than one results from the increased electromagnetic field strength in the ethylene glycol solution compared to that in water. Our observed ratio is comparable to the absorption ratio observed for an aromatic amino acid in a relatively hydrophobic protein environment compared to that in an exposed, predominantly aqueous, environment.<sup>46</sup>

Using the refractive indices discussed above we calculate a value of 1.40 for the ratio of the Raman intensity of NATYR in 90% ethylene glycol: 10% water compared to that in water. This value is somewhat larger than our measured value of 1.28. In addition to the effect of the local field, other specific environmental interactions can modify the absorbances such as hydrogen bonding.<sup>47-49</sup> Furthermore, effects such as differences in the inhomogeneous broadening in the two environments can also affect the ratio of the molar absorptivities.

Large changes in the Raman intensities can occur for aromatic amino acids in different protein environments.<sup>46</sup> For example, if the environment of an aromatic amino acid were highly polarizable as a result of numerous surrounding aromatic amino acids, such that the local refractive index were 2.0, we would calculate a Raman intensity ratio of 5.42 compared to that in water. This increased Raman intensity would appear as an increased Raman cross section if the internal standard used were restricted to the water environment. In contrast, if the internal standard were also localized in the same refractive index environment no change in the relative intensities would be observed and the Raman cross section would appear unchanged.

The large changes in the Raman intensities due to refractive index changes indicate that the Raman intensities are a sensitive monitor of the environmental refractive index. However, the use of Raman intensities to monitor analyte environment will be complicated, because independent changes also occur in the  $\lambda_{\max}$  and absorption band shapes due to specific interactions such as hydrogen bonding. This, of course, will modify the Raman excitation profile bandshape and shift the peak.

Our conclusions that we observe a 23% change in the Tyr<sup>-</sup> Raman intensities due to environmental refractive index changes between water and 90% ethylene glycol assumes that the Raman cross sections are otherwise unchanged for Tyr<sup>-</sup> between these two solvents for excitation of the Raman spectra at the absorption maxima. If the cross sections were to change, due to alterations in the homogeneous or inhomogeneous linewidths, it would, of course, confound our analysis. It is impossible to experimentally examine the environmental refractive index Raman cross sec-

tion dependence without altering the identity of the solvent environment. The modest changes in the absorption spectrum between the pure water and 90% ethylene glycol–10% water solution, however, make it likely that we are observing the local field effect. Whatever the case the environmental change between these two solvents clearly causes a *large* change in the Raman intensity measured at the absorption and excitation profile maxima.

## CONCLUSIONS

We have developed a new Raman spectroscopic technique which can be used to determine relative Raman intensities as a function of the liquid medium refractive index by using teflon as an external standard. The refractive index dependence of the solid angle of light collection disappears in our sampling geometry and the self-absorption bias is minimized. We observe a refractive index dependence for the Raman intensity for *N*-acetyl-*L*-tyrosinamide (NATYR) similar to that we calculate using previously derived expressions which determine the effect of the refractive index on the electromagnetic field strength and upon the Raman scattering. This resulting dependence gives a ca. 25% increased resonance Raman intensity of NATYR in ethylene glycol compared to water for ca. 243 nm excitation. The strong dependence of the Raman intensity upon the local environment suggests that UV resonance Raman intensity measurements can be used to monitor the average environmental refractive index of aromatic amino acids in proteins.

## ACKNOWLEDGMENTS

We gratefully acknowledge Joyce Sweeney's work in designing the cell used for these studies. Helpful discussions with Professor Paul Champion from the Physics Department of Boston University and support of this work from NIH Grant No. IR01GM37041-09.

<sup>1</sup> S. A. Asher, *Annu. Rev. Phys. Chem.* **39**, 537 (1988), and references therein.

<sup>2</sup> A. B. Myers and R. A. Mathies, in *Biological Applications of Raman Spectrometry*, edited by T. G. Spiro (Wiley, New York, 1987), Vol. II, pp. 1–58.

<sup>3</sup> C. R. Johnson, M. Ludwig, S. O'Donnell, and S. A. Asher, *J. Am. Chem. Soc.* **106**, 5008 (1984).

<sup>4</sup> S. A. Asher, M. Ludwig, and C. R. Johnson, *J. Am. Chem. Soc.* **108**, 3186 (1986).

<sup>5</sup> R. P. Rava and T. G. Spiro, *J. Phys. Chem.* **89**, 1856 (1985).

<sup>6</sup> S. P. A. Fodor, R. P. Rava, T. R. Hayes, and T. G. Spiro, *J. Am. Chem. Soc.* **107**, 1520 (1985).

<sup>7</sup> J. M. Dudik, C. R. Johnson, and S. A. Asher, *J. Phys. Chem.* **89**, 3805 (1985).

<sup>8</sup> L. C. Mayne, L. D. Ziegler, and B. S. Hudson, *J. Phys. Chem.* **89**, 3395 (1985).

<sup>9</sup> (a) R. P. Rava and T. G. Spiro, *Biochem.* **24**, 1861 (1985); (b) R. A. Copeland, S. Dasgupta, and T. G. Spiro, *J. Am. Chem. Soc.* **107**, 3370 (1985).

<sup>10</sup> J. A. Sweeney and S. A. Asher, *J. Phys. Chem.* **94**, 4784 (1990).

<sup>11</sup> (a) S. Song, S. A. Asher, S. Krimm, and J. J. Bandekar, *J. Am. Chem. Soc.* **110**, 8547 (1988); (b) S. Song and S. A. Asher, *ibid.* **111**, 4295 (1989).

<sup>12</sup> M. Ludwig and S. A. Asher, *J. Am. Chem. Soc.* **110**, 1005 (1988).

<sup>13</sup> S. A. Asher and J. L. Murtaugh, *Appl. Spectrosc.* **42**, 83 (1988).

<sup>14</sup> (a) J. Teraoka, P. Harmon, and S. A. Asher, *J. Am. Chem. Soc.* **112**, 2892 (1990); (b) C. R. Johnson, M. Ludwig, and S. A. Asher, *ibid.* **108**, 905 (1986); (c) P. A. Harmon, J. Teraoka, and S. A. Asher, *ibid.* **112**, 8789 (1990).

<sup>15</sup> I. Harada and H. Takeuchi, in *Spectroscopy of Biological Systems*, edited by R. J. Clark and R. E. Hestor (Wiley, New York, 1986), Chap. 3.

<sup>16</sup> H. Takeuchi, N. Watanabe, Y. Satoh, and I. Harada, *J. Raman Spectrosc.* **20**, 233 (1989).

<sup>17</sup> M. N. Siamwiza, R. C. Lord, M. C. Chen, T. Takamatsu, I. Harada, H. Matsuura, and T. Shimanouchi, *Biochem.* **14**, 4870 (1975).

<sup>18</sup> G. Liu, C. A. Grygon, and T. G. Spiro, *Biochem.* **28**, 5046 (1989).

<sup>19</sup> P. G. Hildebrandt, R. A. Copeland, T. G. Spiro, J. Otlewski, M. Laszkowski, and F. G. Pendergast, *Biochem.* **27**, 5426 (1988).

<sup>20</sup> J. M. Dudik, C. R. Johnson, and S. A. Asher, *J. Chem. Phys.* **82**, 1732 (1985).

<sup>21</sup> H. W. Schrotter and H. W. Kochner, in *Topics in Current Physics*, edited by A. Weber (Springer, Berlin, 1979), p. 23.

<sup>22</sup> N. Abe, M. Wakayama, and M. Ito, *J. Raman Spectrosc.* **6**, 38 (1977).

<sup>23</sup> K. T. Schomacker, J. K. Delaney, and P. M. Champion, *J. Chem. Phys.* **85**, 4240 (1986).

<sup>24</sup> M. O. Trulson and R. A. Mathies, *J. Chem. Phys.* **84**, 2068 (1986).

<sup>25</sup> B. Li and A. B. Myers, *J. Phys. Chem.* **94**, 4051 (1990).

<sup>26</sup> G. Eckhardt and W. G. Wagner, *J. Mol. Spectrosc.* **19**, 407 (1966).

<sup>27</sup> (a) P. Mirone, *Spectrochim. Acta* **22**, 1897 (1966); (b) P. Mirone, *Chem. Phys. Lett.* **4**, 323 (1969); (c) G. Fini, P. Mirone, and P. Petella, *J. Mol. Spectrosc.* **28**, 144 (1968).

<sup>28</sup> (a) J. R. Nestor and E. R. Lippincott, *J. Raman Spectrosc.* **1**, 305 (1973); (b) J. R. Nestor, Ph.D. thesis, University of Maryland, 1972.

<sup>29</sup> P. A. Harmon and S. A. Asher, *J. Chem. Phys.* **93**, 3094 (1990).

<sup>30</sup> S. A. Asher, C. R. Johnson, and J. Murtaugh, *Rev. Sci. Instrum.* **54**, 1657 (1983).

<sup>31</sup> G. Maret and P. E. Wolf, *Physica A* **157**, 293 (1989).

<sup>32</sup> L. R. Painter, R. D. Birkhoff, and E. T. Arakawa, *J. Chem. Phys.* **51**, 243 (1969).

<sup>33</sup> R. D. Birkhoff, R. N. Hamm, W. W. Williams, E. T. Arakawa, and L. R. Painter, in *Proceedings of the Advanced Study Institute, held under the Auspices of NATO and the Royal Society of Canada-Chemical Spectroscopy and Photochemistry in the Vacuum-Ultraviolet*, edited by C. Sandorfy, P. J. Ausloos, and M. B. Robin (Reidel, Dordrecht, 1974), pp. 129–147.

<sup>34</sup> J. J. Hermans and S. Levinson, *J. Opt. Soc. Am.* **41**, 460 (1951).

<sup>35</sup> F. J. Busselle, N. D. Haig, and C. Lewis, *Chem. Phys. Lett.* **88**, 128 (1982).

<sup>36</sup> M. D. Ediger, R. S. Moog, S. G. Boxer, and M. D. Fayer, *Chem. Phys. Lett.* **88**, 123 (1982).

<sup>37</sup> F. J. Busselle, N. D. Haig, and C. Lewis, *Chem. Phys. Lett.* **88**, 128 (1982).

<sup>38</sup> J. V. Morris, M. A. Mahaney, and J. R. Huber, *J. Phys. Chem.* **80**, 969 (1976).

<sup>39</sup> C. J. F. Bottcher, V. C. Van Belle, P. Bordewij, and A. Rip, in *Theory of Electric Polarization* (Elsevier, Amsterdam, 1973), Vol. I.

<sup>40</sup> L. Onsager, *J. Am. Chem. Soc.* **58**, 1486 (1936).

<sup>41</sup> J. G. Kirkwood, *J. Chem. Phys.* **7**, 911 (1936).

<sup>42</sup> A. B. Myers and R. R. Birge, *J. Chem. Phys.* **73**, 5314 (1980).

<sup>43</sup> D. G. Rea, *J. Opt. Soc. Am.* **49**, 90 (1959).

<sup>44</sup> R. A. MacRae, M. W. Williams, and E. T. Arakawa, *J. Chem. Phys.* **61**, 861 (1974).

<sup>45</sup> B. L. Sowers, E. T. Arakawa, and R. D. Birkhoff, *J. Chem. Phys.* **54**, 2319 (1971).

<sup>46</sup> P. J. Larkin, J. Teraoka, and S. A. Asher, *Biochem.* (submitted).

<sup>47</sup> A. P. Demchenko, in *Ultraviolet Spectroscopy of Proteins* (Springer, Berlin, Heidelberg, New York, 1986).

<sup>48</sup> J. E. Bailey, G. H. Beaven, D. A. Chignell, and W. B. Gratzer, *Eur. J. Biochem.* **1**, 5 (1968).

<sup>49</sup> H. Grinspan, J. Birnbaum, and J. Feitelson, *Biochim. Biophys. Acta* **126**, 13 (1966).